

Central European Journal of Chemistry

Capillary electrophoretic separation and characterizations of CdSe quantum dots

Research Article

Sławomir Oszwałdowski^{a*}, Katarzyna Zawistowska^a, Laura K. Grigsby^b, Kenneth P. Roberts^b

> ^aFaculty of Chemistry, Department of Analytical Chemistry, Warsaw University of Technology, 00-664 Warsaw, Poland

> > ^bDepartment of Chemistry and Biochemistry, The University of Tulsa, Tulsa, OK 74104, USA

Received 29 January 2010; Accepted 23 March 2010

Abstract: We have developed a capillary electrophoresis method to characterize the QD surface ligand interactions with various surfactant systems. The method was demonstrated with 2–5 nm CdSe nanoparticles surface-passivated with trioctylphosphine oxide (TOPO). Water solubility was accomplished by surfactant-assisted phase transfer via an oil-in-water microemulsion using either cationic, anionic, or non-ionic surfactants. Interaction between the QD surface ligand (TOPO) and the alkyl chain of the surfactant molecule produces a complex and dynamic surface coating that can be characterized through manipulation of CE separation buffer composition and capillary surface modification. Additional characterization of the QD surface ligand interactions with surfactants was accomplished by UV-VIS spectroscopy, photoluminescence, and TEM. It is anticipated that studies such as these will elucidate the dynamics of QD surface ligand modifications for use in sensors.

Keywords: Nanoparticles • Size separation • Dynamic coating • Capillary electrophoresis • Surfactant coated CdSe nanoparticles

© Versita Sp. z o.o.

1. Introduction

Semiconductor nanoparticles, also known as quantum dots (QDs), possess unique optical properties having potential use in electrooptic and photonic devices. In particular, efforts have focused on using photoluminescent QDs as probes for chemical and biological sensing [1]. In each case, modification of the QD surface was crucial. For bioassays, the surface modification provides water solubility and reactivity toward *e.g.* antibodies. Several modification strategies have been developed for immunoassays, single molecule tracking, and live-cell and tissue imaging [1-3].

However, the chemistry of QD surface modifications is not well known. This is in part due to the lack of appropriate characterization methods, especially in solution. Specialized techniques such as high-resolution electron energy loss spectroscopy, extended x-ray

absorption fine structure, x-ray absorption near edge structure, and x-ray excited optical luminescence are well-suited for this application, due to their sensitivity to electronic densities of states and local structure [4]. However, these approaches are non-routine and often require a synchrotron source and/or ultra-high vacuum. Thus, the majority of routine QD characterizations rely on UV-Vis absorbance, dynamic light scattering, photoluminescence, and, most commonly, TEM. Although UV-Vis is the simplest method for estimating QD size [5], it is also susceptible to interference from background reagents and impurities and is best suited for very pure QD solutions. Although less routine, TEM is the mainstay for determining QD size. However, TEM imaging can be limited due to the low charge density of semiconducting QDs, poor depth resolution, and difficulties in correlating TEM results with solution behavior. TEM has been shown to be insensitive to alterations of the QD surface chemistry [6].

Dynamic light scattering (DLS) has been shown to be sensitive to nanoparticle size changes during surface ligand exchange; however, little more than particle size and solvation radius can be obtained [6]. Moreover, in addition to particle diameter and surface modification determinations, elucidating surface reactivity and stability are necessary for sensor development. For example, characterization surface charge density and effective hydrodynamic radii may provide insight and control over properties such as diffusion coefficients, solution stability, luminescence quantum efficiency, and even cytoxicity.

One of their most attractive optical properties is the narrow, distinctive emission spectra originating from QDs that can differ by only a nanometer in diameter. Thus, developing routine separation methods capable of resolving QDs of similar size would be valuable for a host of quality control measurements, subsequent QD surface modifications, and for quantifiable QDs sensor responses.

Capillary electrophoresis (CE) is a potentially valuable tool for the above due to its high separation efficiency, open-tubular separation capillary; nanoliter sample volumes; and ease of integration with quantitative detection methods. The migration behavior can be directly related to properties such as particle diameter and surface chemistry (e.g. charge, hydrophobicity, etc.). CE can be employed to separate a variety of nanoparticle types [7-13]. The earliest reports focused on the separation of colloidal Au, Ag, or Ag/Au (core/ shell) nanoparticles. It was shown, for example, that separation of water-soluble Ag/Au water-soluble nanoparticles could be achieved in the micellar mode (MEKC) of CE [10,11]. More recently, it has been shown that CE can characterize and separate semiconducting QDs after surface modification [9,12,14-19]. Capillary zone electrophoresis (CZE) has also been useful to monitor QD surface ligand exchange for water solubility and surface reactivity towards biomolecules (e.g. streptavidin/biotin) [16]. Capillary gel electrophoresis (CGE) has been shown to provide size resolution of CdTe QDs that differ by only 2.6 nm in diameter [9]. However, other than the CGE method of filling the separation capillary with viscous polymer, little has been shown for their routine CZE or MEKC size separation.

It is generally accepted that nanoparticles charge-tosize ratio governs their migration in an applied electric field. Using Au particles of core diameters between 5.2 and 14.6 nm, Schnabel et al. showed with that their migration can be described by

$$\mu = \frac{\zeta \cdot \varepsilon \cdot \varepsilon_0}{1.5\eta} f(\kappa a) \tag{1}$$

where ζ is the zeta potential, ϵ the dielectric constant, ε_0 , the permittivity of vacuum, η the solution viscosity and f(κa) a dimensionless function of κa (the ratio of the radius of the core particle to the electrical double-layer thickness) [13]. Under the same separation conditions, the migration rate depends on the zeta potential as well as size; however, the size dependence would appear limited as f(ka) only varies from 1 to 1.5. Likewise, the influence of zeta potential on resolution and efficiency also appears limited as the ζ potentials were found to be similar (in the range of -23.1 to -25.3 mV) for various size nanoparticles possessing charged surface ligands (e.g. DHLA, dihydrolipoic acid), [6]. Thus, separation of nanoscale particles can be difficult using conventional CE, and additional factors in the separation are needed.

In the present work, a novel approach to QD nanoparticles CZE and MEKC separation and characterization was developed. CdSe nanoparticles surface-passivated with hydrophobic trioctylphosphine oxide (TOPO) were evaluated under aqueous CE conditions. This required using the common technique of rendering the hydrophobic surface ligands water soluble by forming a bilayer with ionic and non-ionic long-chain hydrocarbon surfactants. The dynamic surface coating allowed QD separation and surface characterization by aqueous CZE and MEKC. Such an approach is especially interesting as the intersection between colloid and separation sciences, which were the subject of our previous reports [20,21].

2. Experimental Procedure

2.1 Instrumentation

For photoluminescence measurements, a Safire (Tecan Systems Inc., San Jose, CA) instrument was used. The excitation wavelength was 450 nm and the PL spectra were collected over 480 - 740 nm. UV-Vis measurements were conducted with a HP8453 UV-VIS spectrophotometer with HP ChemStation software (Hewlett-Packard, Palo Alto, CA), using a 1 cm cuvette. TEM measurements were conducted on a Hitachi H 7000 (Hitachi, Japan) system operating at 90 kV.

A P/ACE MDQ CE system (Beckman Coulter, Fullerton, CA) with photo-diode array (PDA) detection was used. An IBM PC and Beckman 32 Karat 5.0 software controlled the CE instrument and acquired the data. A capillary electrophoretic system with UV–VIS detector (Prince Technologies, Holland) was also used (Warsaw lab). Fused-silica capillaries with 75 µm inner diameter were purchased (Polymicro Tech., Phoenix, AZ). The capillary length (window/total length) was

60/70 cm. Prior to daily use, the capillary was pretreated by flushing sequentially for 15 min with 0.1 M NaOH, 5 min with water, and 5 min with run buffer. The capillary was also rinsed with 0.1 M NaOH (5 min), water (3 min), and buffer (5 min) between each run. The injection was typically performed at 35 mbar for 5 s. The separation capillary was temperature controlled at 25°C by liquid cooling of the P/ACE MDQ instrument.

2.2 Chemicals and reagents

All chemicals and reagents were of analytical grade. For the synthesis of the TOPO coated CdSe nanoparticles, cadmium oxide (~1 micron, 99.5%), selenium powder (100 mesh, 99.999%), trioctylphosphine oxide (TOPO, 90%), hexadecylamine (HDA), tributylphosphine (TBP, 97%) trioctylphosphine (TOP, 90%), SDS (sodium dodecyl sulfate), CTAB (cetyltrimethylammonium bromide), LA (sodium laureate), N-101 (Triton N-101, polyoxyethylene nonylcyclohexyl ether), Triton X-100 (polyethylene glycol tert-octylphenyl ether), and sodium tetraborate were obtained from Sigma-Aldrich (St. Louis, MO). The CdSe/DHLA QDs (water soluble, 10 mg mL $^{-1}$, $\lambda_{\rm max}$ 600 nm) were purchased from NANOCO (Manchester, UK).

Aqueous ionic surfactant solutions in the range 10–700 mM and non-ionic Triton (N-101, TX-100; 10% w/w) were prepared. Sudan III was prepared by saturating the dye in 0.5 M SDS and centrifuging (10.000 rpm/5 min). A running buffer of 20 mM sodium tetraborate was used for zone CE separation.

2.3 Preparation of TOPO coated CdSe nanoparticles

Hydrophobic TOPO-coated CdSe nanoparticles were prepared from cadmium oxide and elemental selenium [22]. Briefly, the selenium precursor was prepared by combining elementary selenium and TOP or TBP at room temperature. The cadmium precursor was prepared from cadmium oxide, trioctylphosphine oxide (TOPO) and hexadecylamine (HDA); the mixture was heated to 360°C under flowing Ar and the CdO dissolved. The the solution was cooled to 270°C and the selenium stock solution was injected; nanocrystals grew to the desired size at 250°C. The CdSe/TOPO nanoparticles were purified according to [5]. Using this procedure, pure CdSe/TOP/TOPO or CdSe/TBA/TOPO QDs were obtained in the range of 2.4 – 4.3 nm.

2.4. Preparation of surfactant-coated CdSe nanoparticles

A chloroform solution of CdSe/TOPO nanoparticles (200 µL) was added to 800 µL of surfactant solution in a 10 mL beaker. The solution was stirred and heated simultaneously until all chloroform evaporated. The resulting solution was analyzed as described above. The chloroform solutions of CdSe/TOPO QDs used for sample preparation were as follows (mol L-1; size): 2.8×10⁻⁶ (2.4 nm), 4.3×10⁻⁶, 5.4×10⁻⁵ (2.6 nm), 1.6×10⁻⁵ (2.9 nm), 2.3×10⁻⁶ (3.4 nm), and 2.9×10⁻⁶ (4.3 nm). TEM confirmation of nanoparticle size was accomplished by placing one drop of a dilute sample of CdSe/TOPO or CdSe/TOPO//N-101 QD in chloroform on a Formvarcoated copper grid, allowing 20 s to settle, and wicking away the excess with an absorbent tissue. Size distribution analyses of the TEM particle images were performed.

2.5 Separation of surfactant-coated CdSe nanoparticles by capillary electrophoresis

CdSe QDs coated with anionic (SDS), cationic (CTAB) (both typically 100 mM) or non-ionic surfactants prepared according to Section 2.4 were separated using micellar electrolyte buffer containing surfactant (20 – 100 mM SDS or CTAB) and 10 mM sodium tetraborate. Samples of CdSe/TBP/TOPO//SDS and CdSe/TBP/TOPO//N-101 were separated by SDS-based electrolyte buffers (injection from anode side, + 20 kV), whereas samples of CdSe/TBP/TOPO//CTAB were separated using a CTAB buffer (injection from cathode side, -20 kV). Acetone and Sudan III were used as markers to establish the EOF and the micelle migration time (t_{mic}).

To separate mixtures of different sized surfactant-coated QDs, solutions prepared according to Section 2.4 were mixed just prior to injection at the anode. For the separation, 20 mM sodium tetraborate buffer (pH 9.2) and typically + 20 kV voltage were applied. All electropherograms were detected at 214 nm or 330 nm (Section 3.3). QDs were identified by their characteristic diode-array spectra.

3. Results and Discussion

3.1 Preparation and spectral characterization of surfactant-soluble CdSe/TBP/TOPO nanoparticles

CdSe QDs surface-passivated with hydrophobic TOPO ligands were synthesized using two types of crystal growing precursors (Se/TBP and Se/TOP)

[22]. The resultant solutions were first characterized by UV-Vis spectrophotometry (Fig. 1) to obtain QD concentration and diameter, based on the position and extinction coefficient of the first exciton band in the absorbance spectra [5,9,23,24]. These were confirmed by photoluminescence and TEM measurements (see below). The individual CdSe/TBP/TOPO QDs preparations were 2.4, 2.6, 2.9, 3.4, and 4.3 nm.

The literature gives examples of the preparation of surfactant-coated nanoparticles using either anionic or cationic surfactants [25-28]. Individual nanoparticles can be isolated in a surfactant micellar layer for subsequent surface modifications. Based upon details given in the supplement of [27], we analyzed the effects of various surfactant coatings (SDS, CTAB, Triton TX-100, and N-101) on CdSe/TBP/TOPO nanoparticles to optimize solubility and final QD quantum efficiency. In the coating process, CdSe/TBP/TOPO dissolved in chloroform was added to aqueous surfactant solution to form a microemulsion. As chloroform evaporated the nanoparticles transferred into the surfactant solution. The resultant QD solution was examined by UV-Vis, photoluminescence spectroscopy, TEM, and capillary electrophoresis.

Considerable attention was given to minimizing QD aggregation and precipitation during transfer from chloroform into the aqueous surfactant. Insufficient

formation of a microemulsion, improper QD concentration in the microemulsion, and/or ineffective surfactant concentration were the principal causes of instability. Optimization of the amount of nanoparticle solvent (chloroform) was necessary to form a satisfactory emulsion to facilitate phase transfer, as previously observed [26,27]. 150 - 250 µL of chloroform per 800 µL of surfactant solution is sufficient.

Too high a nanoparticle concentration in the organic phase led to aggregation, precluding phase transfer into the surfactant. Aggregation was also observed when both QD and SDS solutions were prepared in chloroform followed by evaporation under vacuum. Attempts to dissolve dry CdSe/TBP/TOPO QDs using 500 mM SDS were also unsuccessful. However, at a QD concentration of 10-6-10-5 M in chloroform, each QD is completely solvated in the emulsion and thus free to associate with surfactant tail groups at the surfactant/chloroform interface. During chloroform evaporation further association and interdigitation of the TOPO surface ligand with the surfactant tail groups was evidenced by the appearance of a stable and transparent QD solution.

Fig. 1 shows the UV-Vis absorbance and photoluminescence spectra of 2.6 nm (CdSe/TBP/TOPO) and 2.9 nm (CdSe/TOP/TOPO) nanoparticles synthesized from Se-TBP (Fig. 1a) and Se-TOP

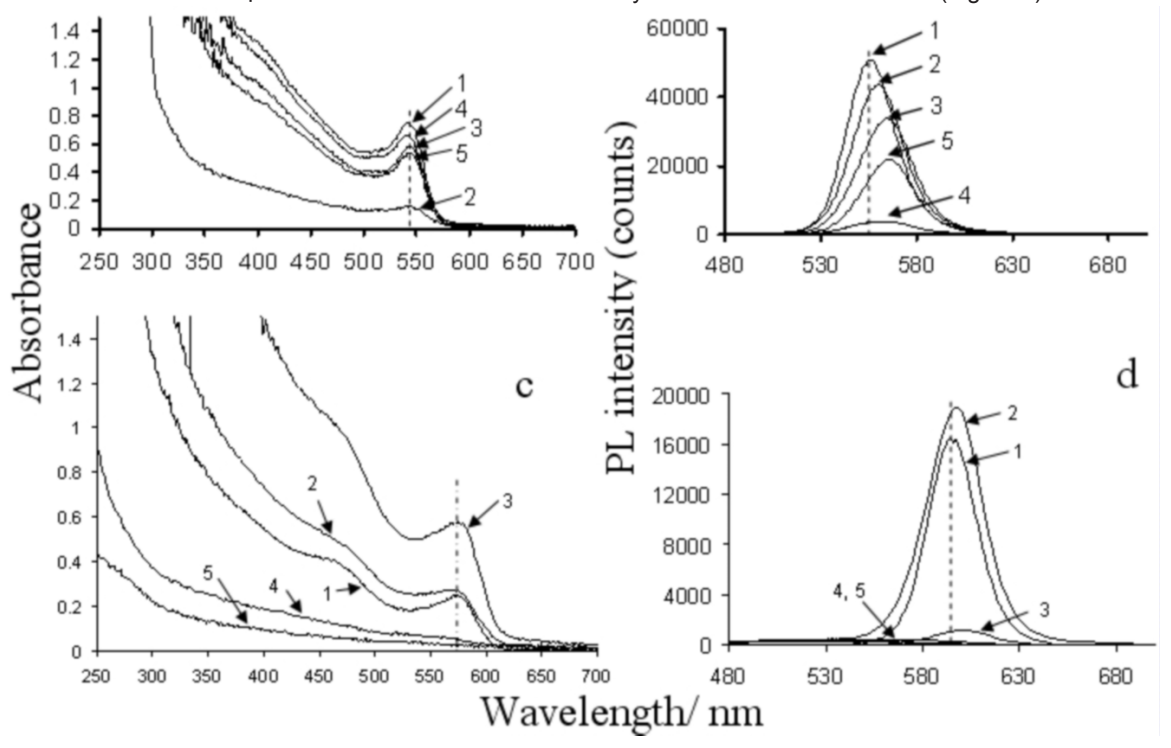


Figure 1. Comparison of CdSe QDs surfactant coating efficiency and coating influence on photoluminescence intensity. Upper (a, b) 2.6 nm CdSe/TBP/TOPO; below (c, d) 2.9 nm CdSe/TOP/TOPO QDs. UV-Vis (a, c) and PL (b, d) spectra were measured on the same sample. Media: 1, chloroform; 2, TX-100 10%; 3, N-101 10%; 4, CTAB 100 mM; and 5, SDS 100 mM. The original sample 4 (upper) was diluted 1:1 with water to reduce the absorbance.

(Fig. 1b) precursors. The spectra were taken in either the original solvent (chloroform) or after transfer to an aqueous phase by coating the QD with cationic, anionic, or non-ionic surfactants. Several conclusions can be drawn. First, CdSe QDs passivated with a mixture of TOPO and TBP have the highest coating efficiency, as shown by the high degree of solubilization and optical absorbance after coating. It was also observed that CdSe/TBP/TOPO QDs were preferentially coated with ionic surfactants (SDS and CTAB), while CdSe/ TOP/TOPO QDs showed selectivity toward non-ionic These showed negligible coating by either anionic or cationic surfactants. In addition, both nanoparticles showed a large dependence on the nonionic surfactant: Triton X-100 was much less effective than N-101 in transferring the QD from the chloroform to the aqueous phase. The coating behavior was generally consistent for all QDs (TBP, TOP) sizes examined.

Corresponding photoluminescence (PL) spectra were also obtained to measure the luminescence quenching caused by the phase transfer. As shown in Figs. 1b and 1d, surfactant-solublized QDs have a bandwidth similar to those for pure CdSe QDs dissolved in organic solvent, in agreement with previous reports [26-28]. The PL spectral shift is related to the QD surface chemistry, as reported previously. The PL intensity for QDs coated with surfactant decreased in order: TX-100 > N-101 > SDS > CTAB, independent of the precursors used or QD size. Luminescence quenching in the CTAB system was very sensitive to surfactant concentration (see Supplementary Fig. 1). The low photoluminescence for concentrations less than 20 mM CTAB was due to the QDs instability in the aqueous medium. At high CTAB concentrations (>100 mM) complete suppression of QD luminescence was observed, although the UV-Vis absorbance spectra remained unchanged by the phase transfer. The latter suggests that no substantial changes to the nanoparticle sizes occurred [5,6,29], as was confirmed by TEM of QDs before and after coating. An example is shown in Supplementary Fig. 2 for 2.9 nm QDs. Nonionic N-101 was used to avoid surfactant crystal formation on the TEM grids.

It has been reported that the observed decreases in photoluminescence intensity can be associated with self-quenching due to incorporation of many QD into the small volume of a single micelle, quenching due to removal of the protective surface TOPO ligand, oxidation of the CdSe core, and/or non-radiative energy loss/transfer to the aqueous surfactant [25,27]. However, as discussed below, capillary electrophoresis results excluded the inclusion of multiple nanoparticles per micelle. Thus, removal of the passivating surface ligands during phase transfer or non-radiative energy transfer were both

considered as mechanisms for quantum yield reduction at high surfactant concentration.

3.2 Separation of QDs by Micellar Electrokinetic Capillary Chromatography

In the previous section, it was established that CdSe/ TBP/TOPO prepared with the Se-TBP precursor could be efficiently coated by ionic or nonionic surfactants. Thus, micellar electrokinetic capillary chromatography (MEKC) separations were performed on CdSe/TBP/ TOPO (denoted further as CdSe/TOPO) QDs to observe the effect of surfactant type on the electrophoretic behavior in an aqueous separation buffer. mode of CE, solutes migrate within a separation time window defined by total inclusion of the solute within the separation micelle $(t_{\rm mic})$ and total exclusion from the micelle at the electroosmotic front (t_{eof}), where the degree of micelle interaction primarily depends on solute hydrophobicity. However, with surfactant-coated QDs, there is superposition of several interdependent surfactant equilibria between: (i) the hydrophobic TBP/ TOPO ligand and the coating, (ii) the QD surface coating and CE separation micelle, and (iii) the micelle and free surfactant in solution.

Presented in this section are MEKC characterizations of the electrophoretic behavior of CdSe/TOPO QDs coated with SDS, CTAB, or N-101 surfactants (denoted as CdSe/TOPO//surfactant). Initial testing was conducted using 2.4 nm QDs coated with SDS (Fig. 2a) and N-101 (Fig. 2c), then separated in 50 mM SDS, with 10 and 1.5 mM sodium tetraborate (pH 9.2). Samples coated with CTAB were characterized using 50 mM CTAB and 10 mM tetraborate (Fig. 2b). For comparison, CdSe/ZnS QDs surface-derivatized with dihydrolipoic acid (DHLA) are also shown. Acetone and Sudan III were added to the coating buffer to define $t_{\rm acf}$ and $t_{\rm mic}$ (Fig. 2d).

As shown in Figs. 2a-c, with a 50 mM SDS or CTAB separation buffer, the migration time of surfactantcoated QDs (t_{OD}) is in the range of the t_{mic} marker Sudan III (position indicated with a dashed line). This indicates that QDs coated with non-ionic (N-101) or ionic (SDS, CTAB) surfactants have electrophoretic and hydrodynamic properties similar to the (SDS or CTAB) separation micelle. Migration near the $t_{\mbox{\tiny mic}}$ could also be due to associations of the surfactant-coated QDs with the separation micelle. However, ionic micelles are only a few nanometers in diameter; thus, size constraints limit or preclude complete penetration of QDs into the micelle interior in the traditional sense. Electrostatic repulsion from the ionic surfactant coating should also limit the degree of micelle - QD interaction. Thus, surfactantcoated QDs (t_{QD}) can be treated as pseudo micelles in

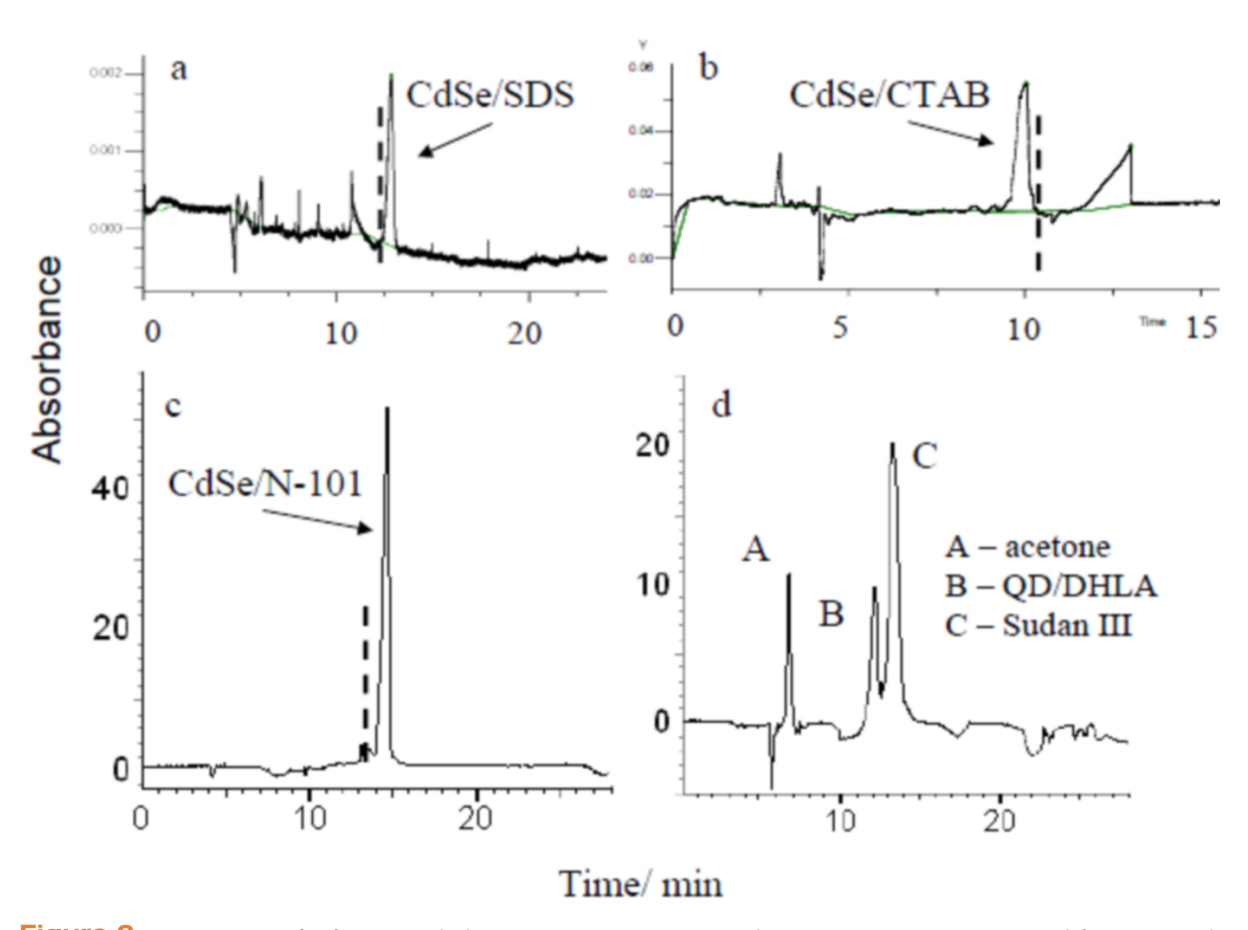


Figure 2. MEKC separation of surfactant coated CdSe/TBP/TOPO QDs: (a) anionic, SDS; (b) cationic, CTAB; (c) non-ionic N-101; (d) for comparison the separation of QD/DHLA QDs in this mode is shown. Separation conditions: electrolyte buffer (a, d) 50 mM SDS/10 mM tetraborate buffer; (c) 50 mM SDS/1.5 mM tetraborate buffer; (b) 50 mM CTAB/10 mM tetraborate buffer. Applied voltage: +20 kV (samples a, b and c), and -20 kV, sample (b). Injections: anode side (samples a, b and c); cathode side (sample b). The dashed lines at (a-c) denote the migration of Sudan III. QDs peaks were confirmed by their characteristic PDA spectra.

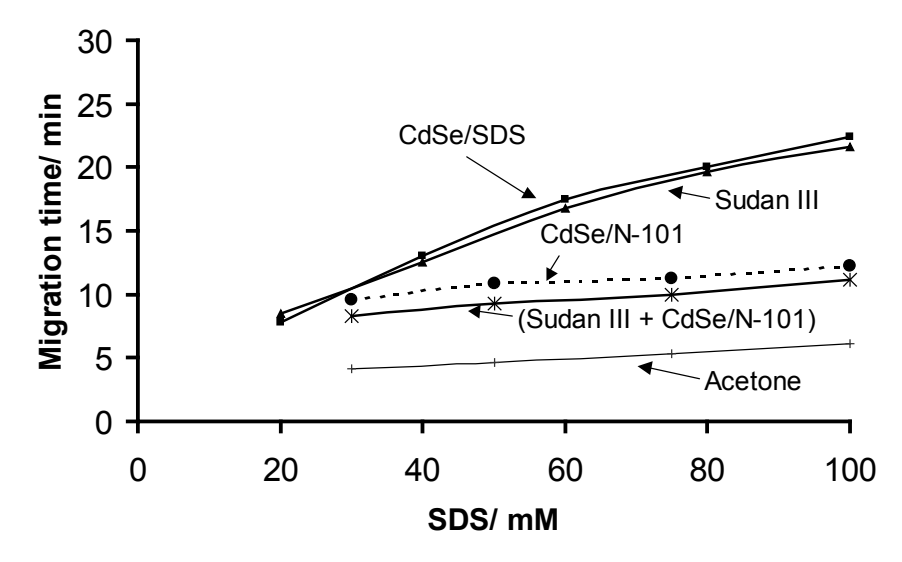


Figure 3. Migration of surfactant modified CdSe/TBP/TOPO QDs at varying surfactant concentration in electrolyte buffer. CdSe/TOPO//SDS, CdSe/N-101 and MEKC markers (acetone and Sudan III). For CdSe/N-101 two peaks were detected (see Section 3.3); the first co-migrated with Sudan III and the position of the second is marked by a dashed line. Electrolyte buffer SDS/ 10 mM or 1.5 mM sodium tetraborate (QDs SDS or N-101 derivative, respectively). Applied voltage: +20 kV for both.

defining their electrophoretic and solution behavior.

Photoluminescence measurements were used to test whether the coating surfactant (*e.g.* N-101, Fig. 2c) exchanges with SDS from the background separation buffer. As shown in Fig. 1, the photoluminescence intensity decreases drastically for QDs coated with SDS surfactant compared to N-101. However, when QDs coated with N-101 were mixed directly with high concentrations of SDS (100 mM), photoluminescence did not decrease for up to two hours. This indicates that N-101 on the QD surface was not replaced with SDS during the 20 minute separation time.

Further insight on the interaction of QDs with the separation surfactant can be obtained by comparing the t_{op} of negatively-charged surfactant-coated QDs (CdSe/TOPO//SDS) to that of QDs that bear a negative charge from exchanging the TOPO surface ligand with dihydrolipoic acid (DHLA). Since both CdSe/TOPO//SDS and CdSe/DHLA are soluble in water and bear a negative surface charge (zeta potential), minimal association with the SDS separation micelle was expected due to charge repulsion. However, as shown in Fig. 2d, the CdSe/ DHLA peak is well resolved from the t_{mic} marker, Sudan III, in contrast to SDS-coated QDs (Fig. 2a). This shift in migration indicates that the negative charge on CdSe/ DHLA aids in shifting the QD equilibrium towards the bulk solution rather than in strong association with the separation micelles and monomers. In contrast, SDS-QDs migrate close to $t_{\mbox{\tiny mic}},$ indicating that the surface either fully retains its initial SDS coating or the coating is in equilibrium with the SDS monomer in the separation buffer.

The effect of MEKC electrolyte buffer surfactant concentration on the migration behavior was tested using SDS-coated 2.4 nm CdSe/TOPO nanoparticles. As described by Khaledi [30], the MEKC surfactant concentration controls both the phase ratio and migration window width. It can be used to adjust the retention factor to improve resolution. As shown in Fig. 3, when the buffer SDS concentration was raised from 20 to 100 mM, $t_{\rm mic}$ (Sudan III) and $t_{\rm QD}$ for SDS-coated QDs overlapped, and no separation was seen. A similar effect was observed for QDs modified with nonionic N-101, which will be discussed below.

The effect of coating surfactant concentration on the electrophoretic behavior of CdSe/TOPO//SDS is shown in Fig. 4. Using separation conditions of 50 mM SDS and 10 mM tetraborate (pH 9.2), as the concentration of the coating surfactant is increased from 30 to 500 mM, the QDs peak shape distorts and broadens.

Concluding from both experiments (Figs. 3, 4), QDs modified by surfactants are incorporated into the micellar zone independent of the MEKC mode

applied. This is due to an interaction between pseudomicelle (QDS/surfactant) and regular surfactant micelle, which regulates the QDs peak shape and separation efficiency.

The separation performance of MEKC for QDs coated in cationic surfactant (CTAB, 100 mM) was also tested using 2.4 and 4.3 nm CdSe/TOPO QDs. Each was tested with a standard CTAB MEKC separation using a separation buffer of 50 mM CTAB with 10 mM sodium tetraborate (pH 9.2) containing up to 25% (v/v) organic modifier (methanol or acetonitrile). Electropherograms a-c in Supplementary Fig. 3 show (a) separation of the t_{mic} marker, (b) 2.4 nm QDs, and (c) 4.3 nm QDs without organic modifier. The large fronting peak at ~ 12 min did not possess a QD absorbance spectrum and was disregarded. However, as can be seen in Supplementary Fig. 3, the 2.4 and 4.3 nm QDs migrate too close to the $t_{\rm mic}$ marker, indicating that their resolution in a mixture would be difficult under these conditions. The secondary peak shown in each electropherogram was a contaminant in the buffer and was not associated with the QD or marker solutions.

Similar results were observed for methanol and acetonitrile content up to 25% (v/v) and for organic modifications of SDS MEKC separations over a range of run buffer concentrations (30–100 mM SDS) using CdSe/TOPO//SDS QDs (data not shown).

3.3 The role of non-ionic surfactants in CdSe QDs electrophoretic separation

MEKC separation of CdSe QD/TOPO/N-101 QDs leads to the appearance of a single typical MEKC peak, a single focused peak, or both (Fig. 5). This is solely due to a QDs N-101 concentration difference injected into the capillary. Additional experiments showed a focused peak for QDs using various non-ionic surfactants (N-101, Fig. 5; TX-100, Supplementary Fig. 4), regardless of the coating surfactant used (non-ionic vs. ionic) or the separation mode (CZE vs. MEKC). Comparisons of CZE and MEKC separations of CdSe QDs coated by ionic surfactant using the non-ionic surfactant TX-100 as focusing agent are included to the Electronic Support Section (Supplementary Fig. 4). Included are accompanying spectra and a blank electropherogram. There are two conclusions. First, the focusing has a great impact on the separation efficiency as measured by number of theoretical plates (N = 5.54[t]/(peak area/peak height,)]2) [31]. The two order of magnitude increase in separation efficiency (Fig. 5) is in agreement with CE/focusing effects for bacteria [8] or metal nanoparticles (reversed electrode polarity stacking) [32,33]. Second, the presence of double peaks during a

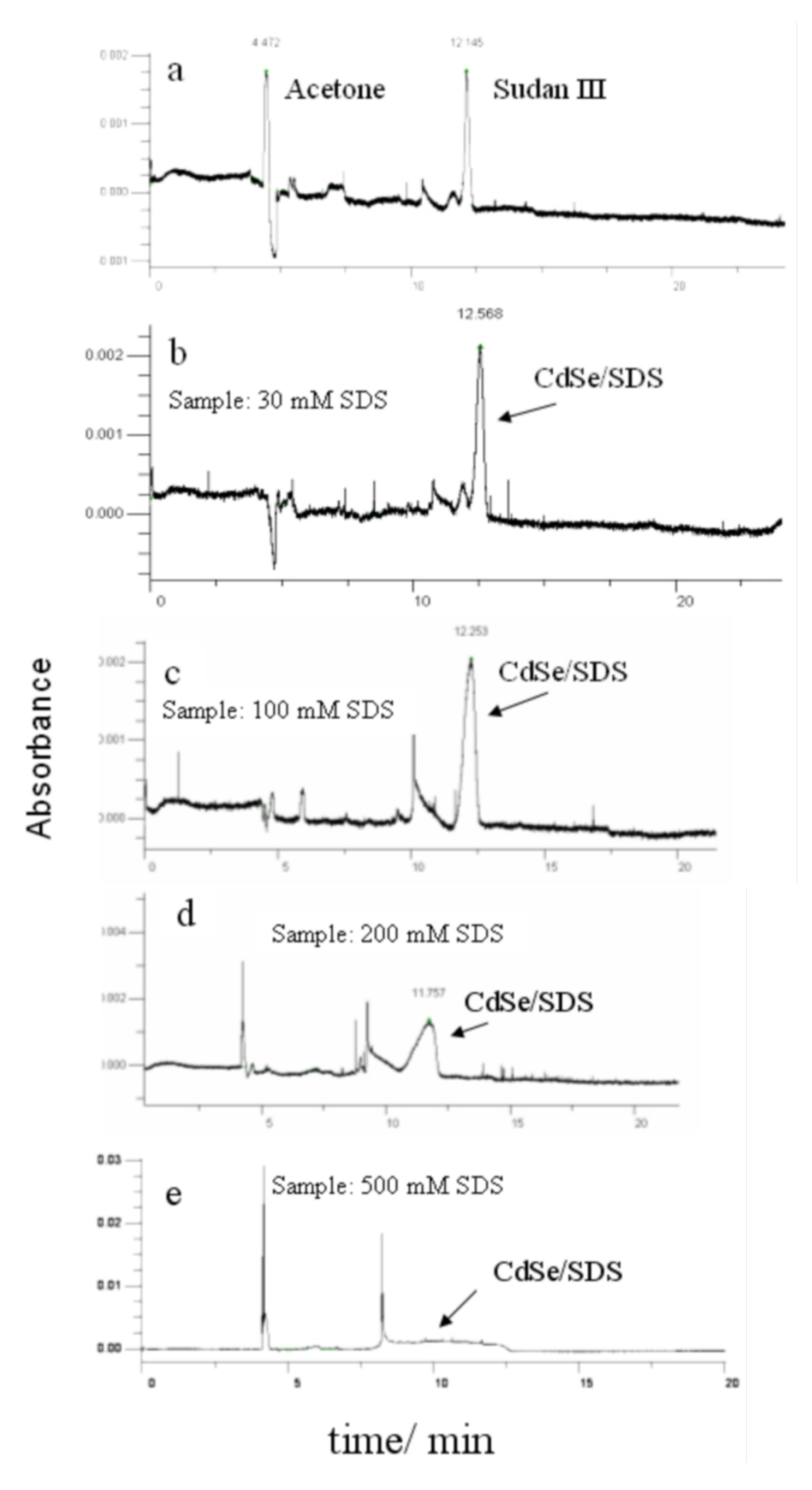


Figure 4. MEKC separation of CdSe/TOPO//SDS QDs at various surfactant (SDS) coating concentrations: (a) migration markers; (b-e) 30 – 500 mM SDS coating concentration. Separation conditions: 50 mM SDS/10 mM sodium tetraborate, applied voltage +20 kV.

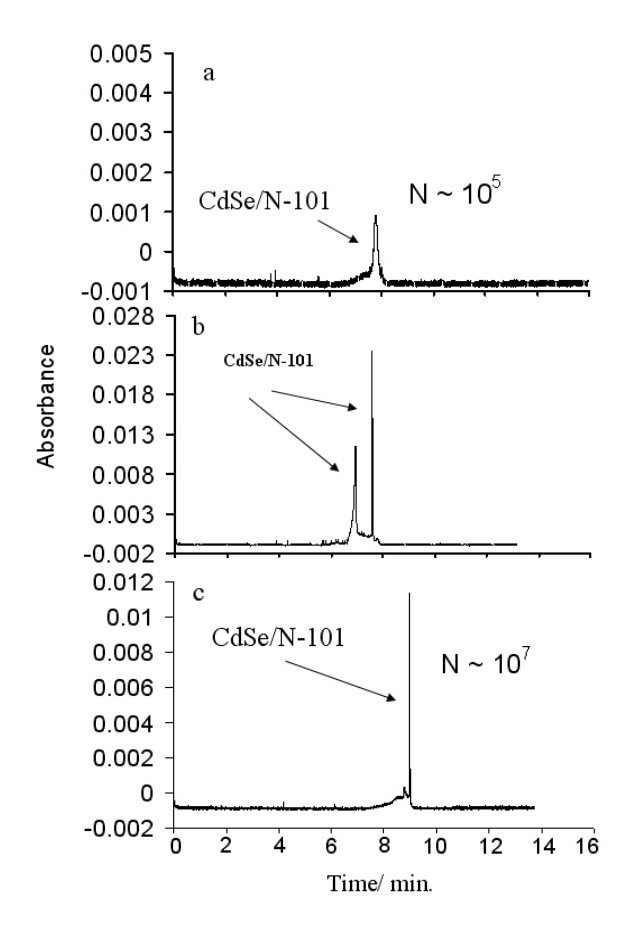


Figure 5. CdSe/N-101 QDs MEKC. (a) 0.5% N-101 (only MEKC peak); (b) 3% N-101 (both MEKC and focused peaks); and (c) 1.5% N-101 (focused peak). Separation conditions: electrolyte buffer 50 mM SDS containing 10 mM sodium tetraborate, applied voltage +20 kV (measured current 40 μA), detection λ = 330 nm. Sample injection: 50 mbar/0.3 min. CdSe/N-101 QDs size, 3.4 nm.

single separation implies the simultaneous presence of two distinct separation mechanisms, which seems to be a new feature in CE separation of QDs (Figs. 5, 6 and Supplementary Fig. 4).

To resolve the final question – whether the MEKC hydrophobic marker Sudan III co-migrates with the first or second QDs peak, additional experiments were done (Fig. 6). Two main separation effects were observed here. The first is an apparent shift in CdSe/N-101 QDs migration depending on the separation mechanism applied. Under the CZE mode, the QDs peak position close to EOF, means that CdSe/N-101 is a polar and uncharged solute. On the other hand, under the MEKC mode, CdSe/N-101 QDs co-migrate with the hydrophobic marker Sudan III. These are apparently contradictory. However, the co-migration of both solutes under MEKC means that QDs migrate as co-surfactants with the surfactant rich micellar zone. This was discussed above. The second issue is that the hydrophobic marker

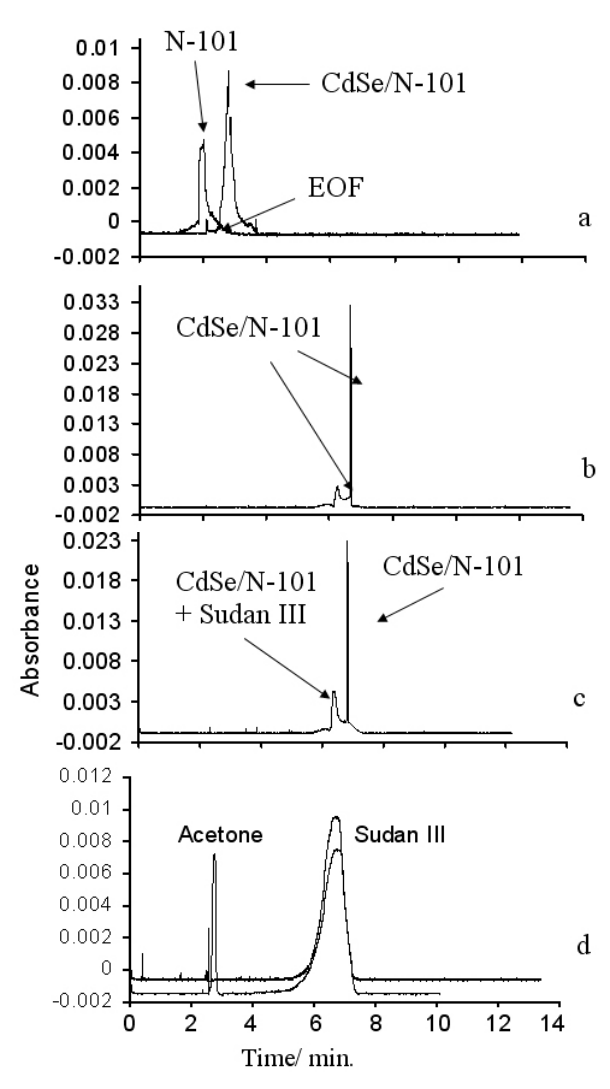


Figure 6. Comparison of CZE and MEKC for the separation of CdSe/N-101 QDs and the peak position for MEKC markers. (a) CZE mode: electrolyte buffer, 20 mM sodium tetraborate; (b-d) MEKC mode: electrolyte buffer, 50 mM SDS containing 10 mM sodium tetraborate. Samples analyzed: (a) sample N-101 (10%) and CdSe/N-101 QDs prepared in 5% N-101 (overlaid); (b) CdSe/N-101 prepared in 1.5% N-101; (c) the same sample as (b) containing Sudan III (95 μL of QDs sample with 5 μL of saturated Sudan III in 0.5 M SDS); (d) acetone and Sudan III markers added to electrolyte buffer (50 mM SDS/10 mM sodium tetraborate) (double injections were shown to confirm the system reliability). Applied voltage for all separations +20 kV. Detection UV-Vis, λ = 330 nm. Sample injection: 50 mbar/0.3 min. CdSe/N-101 QDs size, 3.4 nm.

(Sudan III) did co-migrate with the first CdSe/N-101 peak (MEKC mechanism), whereas the focused peak for QDs was forced to migrate outside the separation window (Fig. 6). The reason for this is the presence of an additional equilibrium or equilibria in the system, but additional studies are needed to drawn more detailed conclusions.

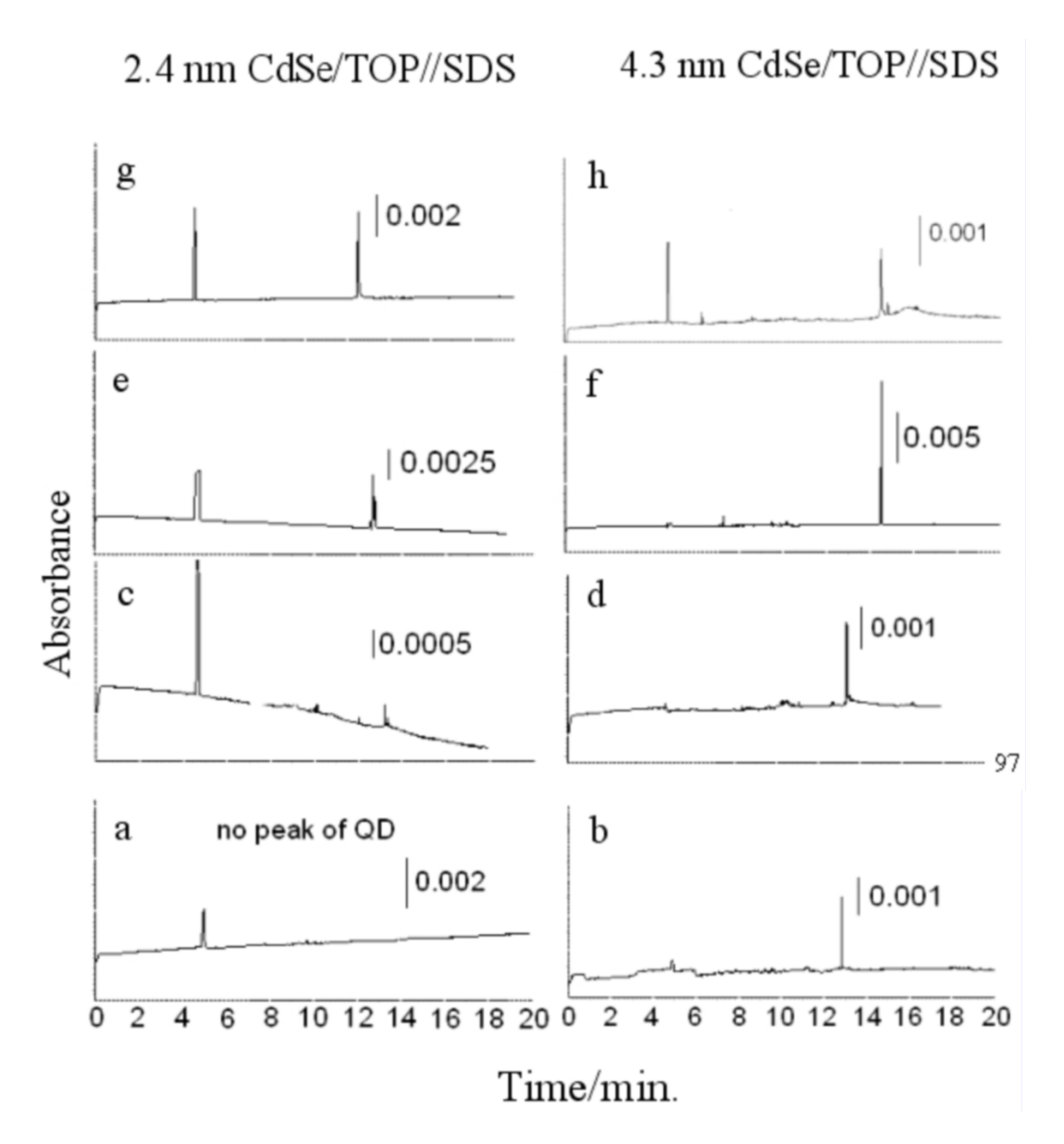


Figure 7. Formation of stable SDS-coated CdSe/TOPO QDs as observed by CZE. Sample preparation: (a, b) 50 mM SDS, no peak was observed for 2.4 nm QD; (c, d) 100 mM SDS; (e, f) 250 mM SDS; (g, h) 500 mM SDS. Sample preparation according to Section 2.4. Run buffer: 20 mM Na₄B₂O₃, applied voltage +20 kV; (a-f) 35 mbar, 5 s; (g, h) 20 mbar, 2 s. The latter was reduced to keep the peak height on scale.

3.4 Characterization of surfactant-coated CdSe/TOPO QDs by Capillary Zone Electrophoresis

In capillary zone electrophoresis (CZE), migration velocities are dependent on particle size, shape, charge, solvation dynamics, and applied field strength. Presented below are preliminary investigations of 2.4 nm CdSe/TOPO under a variety of CZE separation conditions. First, non-aqueous capillary electrophoresis (NACE) was tested using as-prepared CdSe/TOPO QDs. One example of such a separation has been previously reported using 10 mM sodium tetraborate/

EtOH (50%) electrolyte buffer and fluorescence detection [34]. Attempts were made using a variety of typical NACE run buffers based on methanol, ethanol, acetonitrile, chloroform, and their mixtures. Although the hydrophobic nature of CdSe/TOPO QDs should be well suited for NACE separation in organic-based solvents, our attempts were unsuccessful (data not shown) and did not confirm the result in [34]. This suggests that there was non-specific, irreversible binding between the capillary surface and the hydrophobic TOPO surface of the QDs, or the frequently reported dissociation of QD surface ligands [35,36] which can cause precipitation during CE separations.

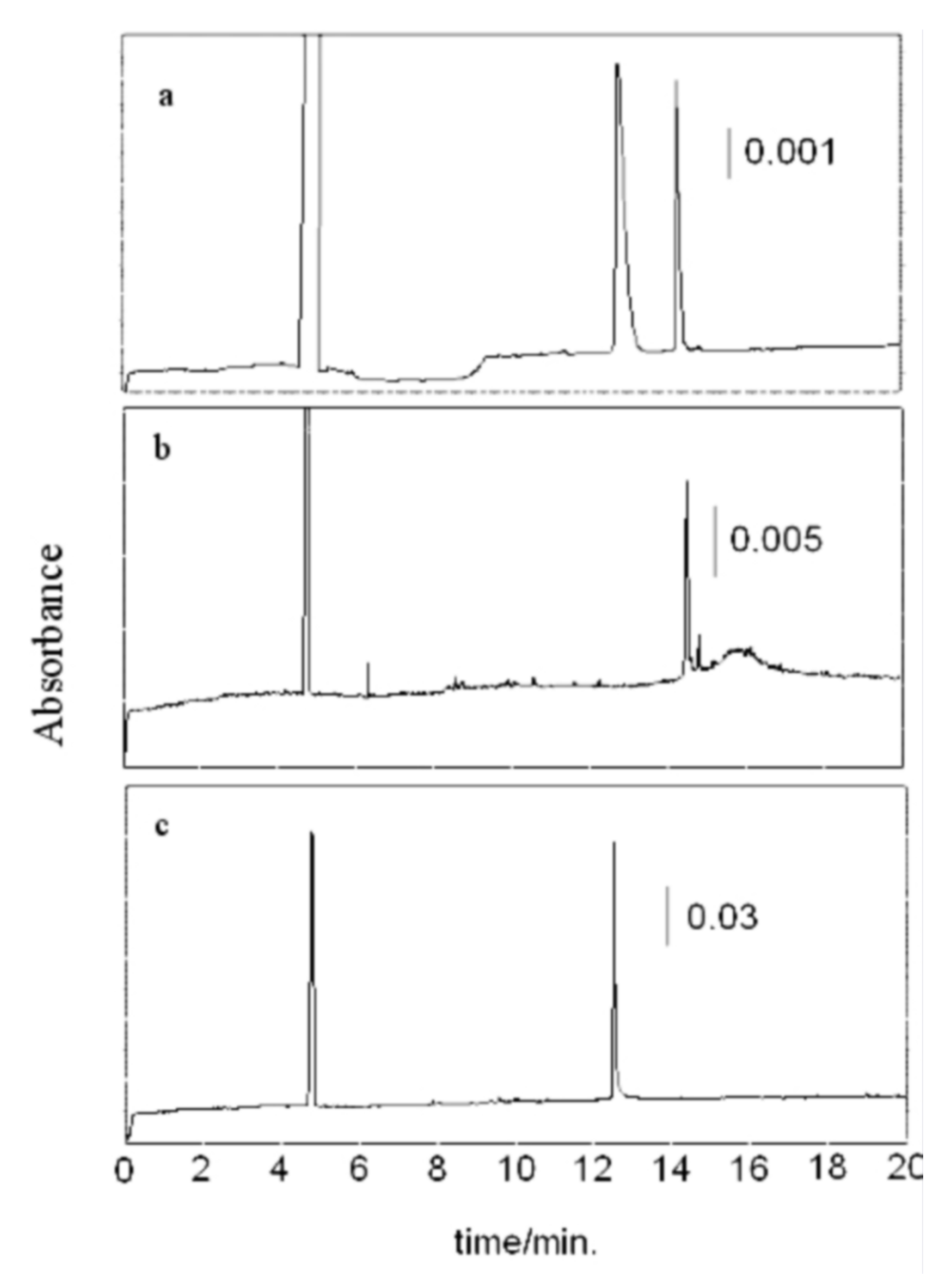


Figure 8. CZE separation of 2.4 nm and 4.3 nm SDS coated CdSe/TOPO QDs. (a) injection of mixture of 2.4 nm and 4.3 QDs (sample: a mixture of 500 mM SDS solutions of QDs; injection 35 mbar, 5 s); (b) injection of 4.3 nm QD; (c) injection of 2.4 nm QD (b and c samples were prepared taking 100 μL of appropriate QD and 0.8 mL 500 mM SDS solution, injection 20 mbar, 2s). Running buffer: 20 mM Na₄B₂O₇, applied voltage +20 kV. QDs were identified by diode-array absorbance spectra (data not shown).

However, separations could be achieved by coating CdSe/TOPO QDs with surfactant prior to injection. The mechanism of separation is likely due to the formation of an electrical double-layer around QDs coated with charged surfactants, allowing them to migrate in the presence of an electrical field without additional MEKC interactions. Example electropherograms are shown in Fig. 7 for SDS-coated 2.4 and 4.3 nm CdSe/

TOPO QDs. Using a 20 mM sodium tetraborate (pH 9.2) CZE buffer, an increase in peak intensity and $t_{\rm QD}$ was observed as the concentration of SDS coating surfactant was increased. The increase in $t_{\rm QD}$ was more pronounced for the larger 4.3 nm QDs; hence, the degree of dynamic coating was a function of size, which provides a mechanism for separating QDs. The effect also confirms the presence of a negative surface charge

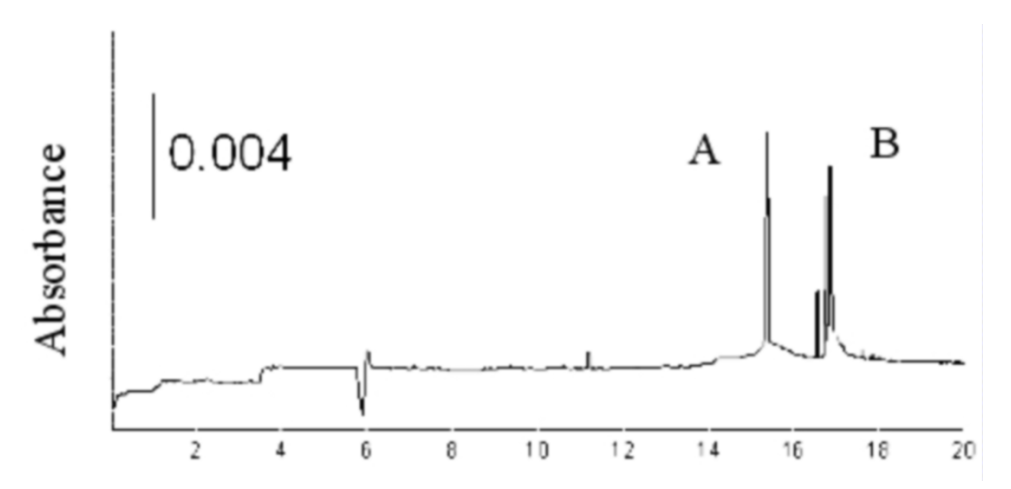


Figure 9. CZE separation of SDS-coated CdSe/ZnS/TOPO QD starting material (A) and DHLA-derivatized product (B). Separation conditions: 20 mM borate buffer, +17 kV.

from the SDS coating as there is agreement between the migration direction and the type of coating. However, the relatively high surfactant concentrations necessary for stable separation suggests that the surfactant may play a dual role in optimizing peak shape, intensity, and $t_{\rm mic}$ in nanoparticle separations. The first role is as a dynamic QD coating agent in agreement with the MEKC results, and second, as an agent for modifying the silica capillary surface. However, in contrast to the MEKC work, excess surfactant in the sample solution did not distort the QD peak shape. This is likely due to more efficient sample focusing in the lower conductivity CZE buffer.

The durability and stability of CdSe/TOPO QDs coated with 500 mM SDS solution were also examined. The smaller surfactant-coated CdSe/TOPO (2.4 nm) QDs were stable for several days, while larger (4.3 nm) particles precipitated in a few hours.

3.5 CZE size separation of surfactant-coated CdSe/TOPO QDs

Previously, the best nanoparticle size resolution was demonstrated for Ag nanoparticles differing in size by 5 nm using MEKC conditions [11]. Further improvement in size resolution was achieved by filling the separation capillary with viscous polymer (capillary gel electrophoresis) which provided separation of QDs differing by 2.6 nm in diameter [9], although replacement of the gel is required between runs.

According to Radko et al. [7], zeta potential $(\zeta \le 25 \text{ mV})$ and mobility are related by:

$$\zeta = \frac{a \cdot \sigma}{\varepsilon \cdot (1 + \kappa a)} \tag{2}$$

where ζ is the zeta potential, a particle radius, σ surface density, and κ is the Debye-Hückel shielding parameter.

In the present work, 20 mM borate buffer was used, thus the 1/k value (electrical double-layer thickness) is equal to 0.68 nm [13]. Under these conditions, the combination of equations 1 and 2 means that the mobility of a charged particle should decrease proportionately to particle size. Such behavior was previously reported, although a simple linear relationship could not be developed [18]. Our results for 2.4 and 4.3 nm CdSe/ TOPO//SDS QDs shown in Fig. 7 agree with the relationship between particle size and migration time. However, although the above suggests that ka is the defining factor for particle migration velocities, since our results used the same buffer and κ regime it is difficult to explain our observed changes in migration by ка alone. According to a previous report, [11] migration of negatively charged gold nanoparticles in a micellar electrolyte buffer depends on the number of adsorbed SDS molecules which is proportional to the surface area. Since the k value was constant under our experimental conditions, nanoparticle charge was added to particle size in interpreting the migration phenomena.

Photoluminescence was also used to aid in characterization of surfactant-coated QD CZE migration. Recalling Supplementary Fig. 1, photoluminescence spectra were obtained as a function of surfactant concentration. An equilibrium exists between hydrophobic TOPO surface ligands and the charged coating surfactant at the nanoparticle surface. This equilibrium depends on size and influences both CE migration (see Fig. 7) and photoluminescence (Supplementary Fig. 1). Varying the amount of charged surface surfactant provides a mechanism for separation by widening the charge-to-size migration window, thus improving QD separations. In this work, 2.4 and 4.3 nm CdSe/TOPO//SDS QDs were chosen to characterize CZE nanoparticle size resolution. As seen in electropherograms a-c of Fig. 8,

the migration of surfactant-coated CdSe/TOPO QDs is a function of size, as shown by the longer migration time for the 4.3 nm nanoparticle.

3.6 Application to QD functionalization

CdSe/TOPO QDs are the basic material for formation of a wide range of functionalized nanoparticles. Traditionally, during the synthesis of functionalized QDs the hydrophobic TOPO/TOP ligands are exchanged with functionalized molecules (e.g. mercaptoacetic acid, dihydrolipoic acid (DHLA), etc.). CZE can be used to separate a mixture of functionalized product and nonfunctionalized starting material. As illustrated in Fig. 9, there is clear separation between the two QDs - with CdSe/DHLA (peak B) migrating much faster than the surfactant-coated CdSe/TOPO (peak A). This indicates that the difference in surface properties (e.g. charge and hydropobicity) plays the main role in the separation of both types of QDs. In addition, the migration order (SDS coated CdSe/TOPO nanoparticles < CdSe/ZnS-DHLA) allows one to estimate that the zeta potential of the SDS coated nanoparticles is below -25 mV, based upon recently published values of zeta potential for CdSe/ ZnS-DHLA QDs [6]. The additional peaks observed in Fig. 9 are due to the aggregation of CdsSe/DHLA QDs during storage, a phenomenon previously reported [7].

References

- [1] I.L. Medintz, H.T. Uyeda, E.R. Goldman, H. Mattoussi, Nat. Mater. 4, 435 (2005)
- [2] O. Carion, B. Mahler, T. Pons, B. Dubertret, Nat. Protocols. 2, 2383 (2007)
- [3] A.R. Clapp, E.R. Goldman, H. Mattoussi, Nat. Protocols. 1, 1258 (2006)
- [4] H. Czichos, T. Saito, L. Smith (Eds.), Springer Handbook of Materials Measurement Methods (Springer-Verlag, Berlin, 2006)
- [5] W.W. Yu, L. Qu, W. Guo, X. Peng, Chem. Mater. 15, 2854 (2003)
- [6] T. Pons, H.T. Uyeda, I.L. Medintz, H. Mattoussi, J. Phys. Chem. B 110, 20308 (2006)
- [7] S.P. Radko, A. Chrambach, Electrophoresis 23, 1957 (2002)
- [8] M.A. Rodriguez, D.W. Armstrong, J. Chromatogr. B 800, 7 (2004)
- [9] X. Song, L. Li, H. Qian, N. Fang, J. Ren, Electrophoresis 27, 1341 (2006)
- [10] F-K. Liu, Y-Y Lin, Ch-H. Wu, Anal. Chim. Acta 528, 249 (2005)
- [11] F-K. Liu, G.T. Wei, Anal. Chim. Acta 510, 77 (2004)

4. Conclusion

The addition of charge to the CdSe/TOPO surface via a surfactant coating provided a suitable tool for CE separation of nanoparticles by size. The capillary electrophoresis results, combined with spectrophotometry and photoluminescence, assist in the characterization of the nanoparticle surface properties in solution. QD separation relies on several dynamic effects, some of which were underscored. Future efforts will focus on elucidating the role each of these factors plays and their importance in the electrophoretic separation of QDs. Supplementary Figures 1-4 are included to the Electronic

Support Section.

Acknowledgements

- the U.S. Air Force Research Laboratory and Air Force Office of Scientific Research - grant number FA9550-06-1-0365,
- Ministry of Science and Higher Education (Poland) - grant number N 204 142837,
- the Office of Research at the University of Tulsa,
- NSF-Oklahoma EPSCoR.
- [12] F-K. Liu, M-H. Tsai, Y-Ch. Hsu, T-Ch. Chu, J. Chromatogr. A 1133, 340 (2006)
- [13] U. Schnabel, Ch-H. Fischer, E. Kenndler, J. Microcol. Sep. 9, 529 (1997)
- [14] X. Huang, J. Weng, F. Sang, X. Song, Ch. Cao, J. Ren, J. Chromatogr. A 1113, 251 (2006)
- [15] H-T. Feng, W-S. Law, L-J. Yu, S.F.-Y. Li, J. Chromatogr. A 1156, 75 (2007)
- [16] G. Vicente, L.A. Colon, Anal. Chem. 80, 1988 (2008)
- [17] M. Pereira, E.P.C. Lai, B. Hollebone, Electrophoresis 28, 2874 (2007)
- [18] U. Pyell, Electrophoresis 29, 576 (2008)
- [19] Ch. Dong, R. Bi, H. Qian, L. Li, J. Ren, Small 2, 534 (2006)
- [20] S. Oszwałdowski, K. Zawistowska, Colloids Surf. A 315, 259 (2008)
- [21] S. Oszwałdowski, A.R. Timerbaev, Electrophoresis 29, 827 (2008)
- [22] Z.A. Peng, X. Peng, J. Am. Chem. Soc. 123, 183 (2001)
- [23] E. Kuçur, F.M. Boldt, S. Cavaliere-Jaricot, J. Ziegler, T. Nann, Anal. Chem. 79, 8987 (2007)

- [24] C. Dushkin, K. Papazova, N. Dushkina, E. Adachi, Colloid Polym. Sci. 284, 80 (2005)
- [25] B. Dubertret, P. Skourides, D. Norris, V. Noireaux, A.H. Brivanlou, A. Libchaber, Science 298, 1759 (2002)
- [26] H. Fan, E.W. Leve, Ch. Scullin, J. Gabaldon, D. Tallant, S. Bunge, T. Boyle, M.C. Wilson, C.J. Brinker, Nano Lett. 5, 645 (2005)
- [27] Z. Zhelev, H. Ohba, R. Bakalova, J. Am. Chem. Soc. 128, 6324 (2006)
- [28] R. Bakalova, Z. Zhelev, I. Aoki, H. Ohba, Y. Imai,I. Kanno, Anal. Chem. 78, 5925 (2006)
- [29] M. Wang, J.K. Oh, T.E. Dykstra, X. Lou, G.D. Scholes, M.A. Winnik, Macromolecules 39, 3664 (2006)
- [30] M.G. Khaledi, J. Chromatogr. A 780, 3 (1997)
- [31] J.P. Landers, Handbook of Capillary Electrophoresis (CRC Press, Danvers, 1997)
- [32] K-H. Lin, T-C. Chu, F-K. Liu, J. Chromatogr. A 1161, 314 (2007)
- [33] F-K. Liu, J. Chromatogr. A 1167, 231 (2007)
- [34] S. Chen, B-F. Liu, L. Fu, T. Xiong, T. Liu, Z. Zhang, Z-L. Huang, Q. Lu, Y-D. Zhao, Q. Luo, J. Chromatogr. A 1109, 160 (2006)
- [35] J.K. Lorenz, A.B. Ellis, J. Am. Chem. Soc. 120, 10970 (1998)
- [36] G. Kalyuzhny, R.W. Murray, J. Phys. Chem. 109, 7012 (2005)